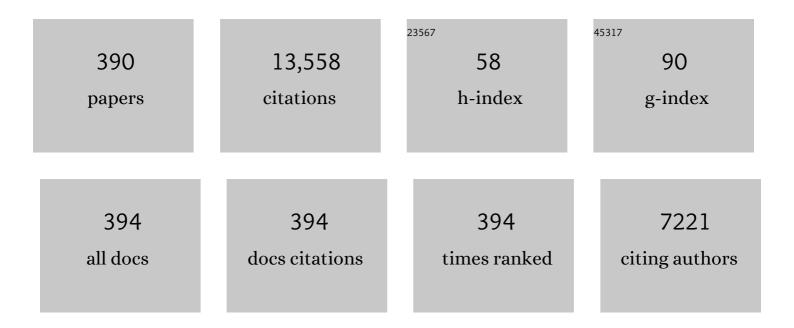
List of Publications by Year in descending order

Source: https://exaly.com/author-pdf/4852669/publications.pdf Version: 2024-02-01



#	Article	IF	CITATIONS
1	Mechanical properties of nanoparticles: basics and applications. Journal Physics D: Applied Physics, 2014, 47, 013001.	2.8	454
2	Double-Walled Carbon Nanotube Solar Cells. Nano Letters, 2007, 7, 2317-2321.	9.1	321
3	Thin film lubrication. Part I. Study on the transition between EHL and thin film lubrication using a relative optical interference intensity technique. Wear, 1996, 194, 107-115.	3.1	270
4	Marangoni flow in an evaporating water droplet. Applied Physics Letters, 2007, 91, .	3.3	248
5	Robust microscale superlubricity under high contact pressure enabled by graphene-coated microsphere. Nature Communications, 2017, 8, 14029.	12.8	235
6	Nanotube–Silicon Heterojunction Solar Cells. Advanced Materials, 2008, 20, 4594-4598.	21.0	210
7	An investigation on the tribological properties of multilayer graphene and MoS2 nanosheets as additives used in hydraulic applications. Tribology International, 2016, 97, 14-20.	5.9	193
8	Evolution of tribo-induced interfacial nanostructures governing superlubricity in a-C:H and a-C:H:Si films. Nature Communications, 2017, 8, 1675.	12.8	179
9	Friction-induced nano-structural evolution of graphene as a lubrication additive. Applied Surface Science, 2018, 434, 21-27.	6.1	175
10	Superlubricity Behavior with Phosphoric Acid–Water Network Induced by Rubbing. Langmuir, 2011, 27, 9413-9417.	3.5	173
11	Superlubricitive engineering—Future industry nearly getting rid of wear and frictional energy consumption. Friction, 2020, 8, 643-665.	6.4	142
12	Ultrathin MoS2 Nanosheets with Superior Extreme Pressure Property as Boundary Lubricants. Scientific Reports, 2015, 5, 12869.	3.3	140
13	Black phosphorus as a new lubricant. Friction, 2018, 6, 116-142.	6.4	136
14	Superlubricity of a graphene/MoS ₂ heterostructure: a combined experimental and DFT study. Nanoscale, 2017, 9, 10846-10853.	5.6	133
15	Macroscale Superlubricity Enabled by the Synergy Effect of Graphene-Oxide Nanoflakes and Ethanediol. ACS Applied Materials & Interfaces, 2018, 10, 40863-40870.	8.0	131
16	Superlubricity Achieved with Mixtures of Acids and Glycerol. Langmuir, 2013, 29, 271-275.	3.5	126
17	CMP of hard disk substrate using a colloidal SiO2 slurry: preliminary experimental investigation. Wear, 2004, 257, 461-470.	3.1	123
18	Interlayer Friction and Superlubricity in Single-Crystalline Contact Enabled by Two-Dimensional Flake-Wrapped Atomic Force Microscope Tips. ACS Nano, 2018, 12, 7638-7646.	14.6	120

#	Article	IF	CITATIONS
19	Robust ultra-low-friction state of graphene via moiré superlattice confinement. Nature Communications, 2016, 7, 13204.	12.8	116
20	Superlubricity of Black Phosphorus as Lubricant Additive. ACS Applied Materials & Interfaces, 2018, 10, 43203-43210.	8.0	113
21	Black Phosphorus: Degradation Favors Lubrication. Nano Letters, 2018, 18, 5618-5627.	9.1	107
22	Self-Assembled Graphene Film as Low Friction Solid Lubricant in Macroscale Contact. ACS Applied Materials & Interfaces, 2017, 9, 21554-21562.	8.0	103
23	Superlubricity of Graphite Induced by Multiple Transferred Graphene Nanoflakes. Advanced Science, 2018, 5, 1700616.	11.2	99
24	Superlubricity of two-dimensional fluorographene/MoS ₂ heterostructure: a first-principles study. Nanotechnology, 2014, 25, 385701.	2.6	98
25	Electrical bearing failures in electric vehicles. Friction, 2020, 8, 4-28.	6.4	97
26	Criterion for Reversal of Thermal Marangoni Flow in Drying Drops. Langmuir, 2010, 26, 1918-1922.	3.5	96
27	A review on tribology of polymer composite coatings. Friction, 2021, 9, 429-470.	6.4	95
28	Origin of friction and the new frictionless technology—Superlubricity: Advancements and future outlook. Nano Energy, 2021, 86, 106092.	16.0	93
29	Superlubricity Achieved with Mixtures of Polyhydroxy Alcohols and Acids. Langmuir, 2013, 29, 5239-5245.	3.5	92
30	Intelligent lubricating materials: A review. Composites Part B: Engineering, 2020, 202, 108450.	12.0	89
31	The Tribological Properties of Oils Added with Diamond Nano-Particles. Tribology Transactions, 2001, 44, 494-498.	2.0	88
32	Macroscale superlubricity under extreme pressure enabled by the combination of graphene-oxide nanosheets with ionic liquid. Carbon, 2019, 151, 76-83.	10.3	86
33	Superlubricity of Graphite Sliding against Graphene Nanoflake under Ultrahigh Contact Pressure. Advanced Science, 2018, 5, 1800810.	11.2	85
34	Tribochemistry and Superlubricity Induced by Hydrogen Ions. Langmuir, 2012, 28, 15816-15823.	3.5	83
35	Synergetic effect of H2O2 and glycine on cobalt CMP in weakly alkaline slurry. Microelectronic Engineering, 2014, 122, 82-86.	2.4	82
36	Ultra-Wear-Resistant MXene-Based Composite Coating via in Situ Formed Nanostructured Tribofilm. ACS Applied Materials & Interfaces, 2019, 11, 32569-32576.	8.0	82

#	Article	IF	CITATIONS
37	Mechanical and tribological properties of nanocomposites incorporated with two-dimensional materials. Friction, 2020, 8, 813-846.	6.4	79
38	Ultrasonic flexural vibration assisted chemical mechanical polishing for sapphire substrate. Applied Surface Science, 2010, 256, 3936-3940.	6.1	77
39	Superlubricity and Antiwear Properties of In Situ-Formed Ionic Liquids at Ceramic Interfaces Induced by Tribochemical Reactions. ACS Applied Materials & amp; Interfaces, 2019, 11, 6568-6574.	8.0	76
40	Elastic Properties of Polystyrene Nanospheres Evaluated with Atomic Force Microscopy: Size Effect and Error Analysis. Langmuir, 2014, 30, 7206-7212.	3.5	75
41	Excellent Lubricating Behavior of Brasenia schreberi Mucilage. Langmuir, 2012, 28, 7797-7802.	3.5	74
42	Nanoconfined ionic liquids under electric fields. Applied Physics Letters, 2010, 96, .	3.3	73
43	1,2,4-Triazole as a corrosion inhibitor in copper chemical mechanical polishing. Thin Solid Films, 2014, 556, 395-404.	1.8	73
44	Thin film lubrication in the past 20 years. Friction, 2016, 4, 280-302.	6.4	70
45	Macroscale Superlubricity Enabled by Hydrated Alkali Metal Ions. Langmuir, 2018, 34, 11281-11291.	3.5	70
46	Effect of ionic strength on ruthenium CMP in H2O2-based slurries. Applied Surface Science, 2014, 317, 332-337.	6.1	69
47	The effect of sulfur on the number of layers in a carbon nanotube. Carbon, 2007, 45, 2152-2158.	10.3	68
48	Effects of the ultrasonic flexural vibration on the interaction between the abrasive particles; pad and sapphire substrate during chemical mechanical polishing (CMP). Applied Surface Science, 2011, 257, 2905-2911.	6.1	66
49	Self-Lubricating PTFE-Based Composites with Black Phosphorus Nanosheets. Tribology Letters, 2018, 66, 1.	2.6	66
50	Synergistic tribological behaviors of graphene oxide and nanodiamond as lubricating additives in water. Tribology International, 2019, 132, 177-184.	5.9	65
51	Optimization of groove texture profile to improve hydrodynamic lubrication performance: Theory and experiments. Friction, 2020, 8, 83-94.	6.4	65
52	Enhancement of friction performance enabled by a synergetic effect between graphene oxide and molybdenum disulfide. Carbon, 2019, 154, 266-276.	10.3	64
53	In-situ formation of tribofilm with Ti3C2Tx MXene nanoflakes triggers macroscale superlubricity. Tribology International, 2021, 154, 106695.	5.9	64
54	A comparative study between graphene oxide and diamond nanoparticles as water-based lubricating additives. Science China Technological Sciences, 2013, 56, 152-157.	4.0	63

#	Article	IF	CITATIONS
55	Friction and wear performance of titanium alloy against tungsten carbide lubricated with phosphate ester. Tribology International, 2016, 95, 27-34.	5.9	63
56	Investigation of the difference in liquid superlubricity between water- and oil-based lubricants. RSC Advances, 2015, 5, 63827-63833.	3.6	62
57	Tribological properties of titanium alloys under lubrication of SEE oil and aqueous solutions. Tribology International, 2017, 109, 40-47.	5.9	62
58	Superlubricity of Polyalkylene Glycol Aqueous Solutions Enabled by Ultrathin Layered Double Hydroxide Nanosheets. ACS Applied Materials & Interfaces, 2019, 11, 20249-20256.	8.0	62
59	Atomic-scale insights into the interfacial instability of superlubricity in hydrogenated amorphous carbon films. Science Advances, 2020, 6, eaay1272.	10.3	61
60	Influence of the micromorphology of reduced graphene oxide sheets on lubrication properties as a lubrication additive. Tribology International, 2018, 119, 614-621.	5.9	60
61	Highly Exfoliated Reduced Graphite Oxide Powders as Efficient Lubricant Oil Additives. Advanced Materials Interfaces, 2016, 3, 1600700.	3.7	59
62	Tribological Behavior of NiAl-Layered Double Hydroxide Nanoplatelets as Oil-Based Lubricant Additives. ACS Applied Materials & Interfaces, 2017, 9, 30891-30899.	8.0	59
63	Liquid Superlubricity of Polyethylene Glycol Aqueous Solution Achieved with Boric Acid Additive. Langmuir, 2018, 34, 3578-3587.	3.5	59
64	Hydrodynamic effect on the superlubricity of phosphoric acid between ceramic and sapphire. Friction, 2014, 2, 173-181.	6.4	58
65	Synthesis of thermally reduced graphite oxide in sulfuric acid and its application as an efficient lubrication additive. Tribology International, 2017, 116, 303-309.	5.9	58
66	Rare earth effect on microstructure, mechanical and tribological properties of CoCrW coatings. Materials Science & Engineering A: Structural Materials: Properties, Microstructure and Processing, 2007, 444, 92-98.	5.6	57
67	Monoatomic layer removal mechanism in chemical mechanical polishing process: A molecular dynamics study. Journal of Applied Physics, 2010, 107, .	2.5	56
68	Lubrication under charged conditions. Tribology International, 2015, 84, 22-35.	5.9	56
69	Rare earth effect on the microstructure and wear resistance of Ni-based coatings. Materials Science & Engineering A: Structural Materials: Properties, Microstructure and Processing, 2007, 454-455, 194-202.	5.6	55
70	Tribochemistry of Phosphoric Acid Sheared between Quartz Surfaces: A Reactive Molecular Dynamics Study. Journal of Physical Chemistry C, 2013, 117, 25604-25614.	3.1	55
71	AFM Studies on Liquid Superlubricity between Silica Surfaces Achieved with Surfactant Micelles. Langmuir, 2016, 32, 5593-5599.	3.5	55
72	Contribution of a Tribo-Induced Silica Layer to Macroscale Superlubricity of Hydrated Ions. Journal of Physical Chemistry C, 2019, 123, 20270-20277.	3.1	55

#	Article	IF	CITATIONS
73	In Situ Green Synthesis of the New Sandwichlike Nanostructure of Mn ₃ O ₄ /Graphene as Lubricant Additives. ACS Applied Materials & Interfaces, 2019, 11, 36931-36938.	8.0	55
74	Advancements in superlubricity. Science China Technological Sciences, 2013, 56, 2877-2887.	4.0	54
75	Tribochemical Mechanism of Amorphous Silica Asperities in Aqueous Environment: A Reactive Molecular Dynamics Study. Langmuir, 2015, 31, 1429-1436.	3.5	54
76	Superlubricity of silicone oil achieved between two surfaces by running-in with acid solution. RSC Advances, 2015, 5, 30861-30868.	3.6	53
77	Tribological behavior of polytetrafluoroethylene coating reinforced with black phosphorus nanoparticles. Applied Surface Science, 2018, 441, 670-677.	6.1	53
78	Macroscale Superlubricity Achieved on the Hydrophobic Graphene Coating with Glycerol. ACS Applied Materials & Interfaces, 2020, 12, 18859-18869.	8.0	51
79	Controllable Superlubricity of Glycerol Solution via Environment Humidity. Langmuir, 2013, 29, 11924-11930.	3.5	50
80	Synergetic effect of benzotriazole and non-ionic surfactant on copper chemical mechanical polishing in KIO4-based slurries. Thin Solid Films, 2014, 558, 272-278.	1.8	50
81	Direct Visualization of Exciton Transport in Defective Few‣ayer WS ₂ by Ultrafast Microscopy. Advanced Materials, 2020, 32, e1906540.	21.0	50
82	Black Phosphorus Quantum Dots in Aqueous Ethylene Glycol for Macroscale Superlubricity. ACS Applied Nano Materials, 2020, 3, 4799-4809.	5.0	50
83	Investigation of running-in process in water-based lubrication aimed at achieving super-low friction. Tribology International, 2016, 102, 257-264.	5.9	49
84	Molecular behaviors in thin film lubrication—Part three: Superlubricity attained by polar and nonpolar molecules. Friction, 2019, 7, 625-636.	6.4	49
85	Macroscale superlubricity of Si-doped diamond-like carbon film enabled by graphene oxide as additives. Carbon, 2021, 176, 358-366.	10.3	48
86	Abrasive rolling effects on material removal and surface finish in chemical mechanical polishing analyzed by molecular dynamics simulation. Journal of Applied Physics, 2011, 109, .	2.5	47
87	Temperature distribution along the surface of evaporating droplets. Physical Review E, 2014, 89, 032404.	2.1	47
88	Numerical optimization of the groove texture bottom profile for thrust bearings. Tribology International, 2017, 109, 69-77.	5.9	47
89	Superlubricity of 1-Ethyl-3-methylimidazolium trifluoromethanesulfonate Ionic Liquid Induced by Tribochemical Reactions. Langmuir, 2018, 34, 5245-5252.	3.5	47
90	Friction and wear behavior of PTFE coatings modified with poly (methyl methacrylate). Composites Part B: Engineering, 2019, 172, 316-322.	12.0	47

#	Article	IF	CITATIONS
91	Origins of Superlubricity Promoted by Hydrated Multivalent Ions. Journal of Physical Chemistry Letters, 2020, 11, 184-190.	4.6	47
92	Tribochemical Behaviors of Onion-like Carbon Films as High-Performance Solid Lubricants with Variable Interfacial Nanostructures. ACS Applied Materials & Interfaces, 2019, 11, 25535-25546.	8.0	46
93	Macroscale Superlubricity Achieved With Various Liquid Molecules: A Review. Frontiers in Mechanical Engineering, 2019, 5, .	1.8	46
94	Super-Slippery Degraded Black Phosphorus/Silicon Dioxide Interface. ACS Applied Materials & Interfaces, 2020, 12, 7717-7726.	8.0	46
95	Mechanism of Biological Liquid Superlubricity of <i>Brasenia schreberi</i> Mucilage. Langmuir, 2014, 30, 3811-3816.	3.5	45
96	Chemical mechanical polishing of steel substrate using colloidal silica-based slurries. Applied Surface Science, 2015, 330, 487-495.	6.1	45
97	Random occurrence of macroscale superlubricity of graphite enabled by tribo-transfer of multilayer graphene nanoflakes. Carbon, 2018, 138, 154-160.	10.3	45
98	Modified graphene as novel lubricating additive with high dispersion stability in oil. Friction, 2021, 9, 143-154.	6.4	45
99	Ultralow friction polymer composites incorporated with monodispersed oil microcapsules. Friction, 2021, 9, 29-40.	6.4	45
100	Ultra-low friction of a-C:H films enabled by lubrication of nanodiamond and graphene in ambient air. Carbon, 2019, 154, 203-210.	10.3	44
101	Tribological properties of rare earth oxide added Cr3C2–NiCr coatings. Applied Surface Science, 2007, 253, 4377-4385.	6.1	43
102	Effect of surface physicochemical properties on the lubricating properties of water film. Applied Surface Science, 2008, 254, 7137-7142.	6.1	43
103	Superlubricity of nanodiamonds glycerol colloidal solution between steel surfaces. Colloids and Surfaces A: Physicochemical and Engineering Aspects, 2016, 489, 400-406.	4.7	43
104	Mechanism of Antiwear Property Under High Pressure of Synthetic Oil-Soluble Ultrathin MoS ₂ Sheets as Lubricant Additives. Langmuir, 2018, 34, 1635-1644.	3.5	43
105	Superlubricity between Graphite Layers in Ultrahigh Vacuum. ACS Applied Materials & Interfaces, 2020, 12, 43167-43172.	8.0	43
106	Fluorinated Graphene: A Promising Macroscale Solid Lubricant under Various Environments. ACS Applied Materials & Interfaces, 2019, 11, 40470-40480.	8.0	42
107	Effects of grain boundary on wear of graphene at the nanoscale: A molecular dynamics study. Carbon, 2019, 143, 578-586.	10.3	42
108	2D metal-organic frameworks with square grid structure: A promising new-generation superlubricating material. Nano Today, 2021, 40, 101262.	11.9	42

#	Article	IF	CITATIONS
109	Effect of substrate morphology on the roughness evolution of ultra thin DLC films. Applied Surface Science, 2008, 254, 6742-6748.	6.1	41
110	Layered Double Hydroxide Nanoplatelets with Excellent Tribological Properties under High Contact Pressure as Water-Based Lubricant Additives. Scientific Reports, 2016, 6, 22748.	3.3	41
111	Mild thermal reduction of graphene oxide as a lubrication additive for friction and wear reduction. RSC Advances, 2017, 7, 1766-1770.	3.6	41
112	Characteristics of Liquid Lubricant Films at the Nano-Scale. Journal of Tribology, 1999, 121, 872-878.	1.9	40
113	Investigations of the superlubricity of sapphire against ruby under phosphoric acid lubrication. Friction, 2014, 2, 164-172.	6.4	40
114	Zwitterionic Hydrogel Incorporated Graphene Oxide Nanosheets with Improved Strength and Lubricity. Langmuir, 2019, 35, 11452-11462.	3.5	40
115	Superlubricity under ultrahigh contact pressure enabled by partially oxidized black phosphorus nanosheets. Npj 2D Materials and Applications, 2021, 5, .	7.9	40
116	Hexadecane-containing sandwich structure based triboelectric nanogenerator with remarkable performance enhancement. Nano Energy, 2021, 87, 106198.	16.0	40
117	Electrochemical investigation of copper passivation kinetics and its application to low-pressure CMP modeling. Applied Surface Science, 2013, 265, 764-770.	6.1	39
118	Preparation and tribological properties of solid-liquid synergetic self-lubricating PTFE/SiO2/PAO6 composites. Composites Part B: Engineering, 2020, 196, 108133.	12.0	39
119	Superlubrication obtained with mixtures of hydrated ions and polyethylene glycol solutions in the mixed and hydrodynamic lubrication regimes. Journal of Colloid and Interface Science, 2020, 579, 479-488.	9.4	39
120	Tribochemical mechanism of superlubricity in graphene quantum dots modified DLC films under high contact pressure. Carbon, 2021, 173, 329-338.	10.3	38
121	The protective properties of ultra-thin diamond like carbon films for high density magnetic storage devices. Applied Surface Science, 2009, 256, 322-328.	6.1	37
122	Investigation of Superlubricity Achieved by Polyalkylene Glycol Aqueous Solutions. Advanced Materials Interfaces, 2016, 3, 1600531.	3.7	37
123	Molecular Origin of Superlubricity between Graphene and a Highly Hydrophobic Surface in Water. Journal of Physical Chemistry Letters, 2019, 10, 2978-2984.	4.6	37
124	Origin of hydration lubrication of zwitterions on graphene. Nanoscale, 2018, 10, 16887-16894.	5.6	36
125	Nano-tribological properties and mechanisms of the liquid crystal as an additive. Science Bulletin, 2001, 46, 1227-1232.	1.7	35
126	Investigation of the running-in process and friction coefficient under the lubrication of ionic liquid/water mixture. Applied Surface Science, 2009, 255, 6408-6414.	6.1	35

#	Article	IF	CITATIONS
127	Functions of Trilon® P as a polyamine in copper chemical mechanical polishing. Applied Surface Science, 2014, 288, 265-274.	6.1	35
128	Microstructure, mechanical and adhesive properties of CrN/CrTiAlSiN/WCrTiAlN multilayer coatings deposited on nitrided AISI 4140 steel. Materials Characterization, 2019, 147, 353-364.	4.4	35
129	Tribo-Induced Interfacial Material Transfer of an Atomic Force Microscopy Probe Assisting Superlubricity in a WS ₂ /Graphene Heterojunction. ACS Applied Materials & Interfaces, 2020, 12, 4031-4040.	8.0	35
130	Tribological behavior of layered double hydroxides with various chemical compositions and morphologies as grease additives. Friction, 2021, 9, 952-962.	6.4	35
131	Investigations on the mechanism of superlubricity achieved with phosphoric acid solution by direct observation. Journal of Applied Physics, 2013, 114, 114901.	2.5	34
132	Interfacial Nanostructure of 2D Ti ₃ C ₂ /Graphene Quantum Dots Hybrid Multicoating for Ultralow Wear. Advanced Engineering Materials, 2020, 22, 1901369.	3.5	34
133	Moiré superlattice-level stick-slip instability originated from geometrically corrugated graphene on a strongly interacting substrate. 2D Materials, 2017, 4, 025079.	4.4	33
134	Synthesis and characterizations of zwitterionic copolymer hydrogels with excellent lubrication behavior. Tribology International, 2020, 143, 106026.	5.9	33
135	Influence Factors on Mechanisms of Superlubricity in DLC Films: A Review. Frontiers in Mechanical Engineering, 2020, 6, .	1.8	33
136	An investigation on the tribological behaviors of steel/copper and steel/steel friction pairs via lubrication with a graphene additive. Friction, 2021, 9, 228-238.	6.4	33
137	Shear-Induced Interfacial Structural Conversion Triggers Macroscale Superlubricity: From Black Phosphorus Nanoflakes to Phosphorus Oxide. ACS Applied Materials & Interfaces, 2021, 13, 31947-31956.	8.0	33
138	Investigation of the film formation mechanism of oil-in-water (O/W) emulsions. Soft Matter, 2011, 7, 4207.	2.7	32
139	Mechanisms for nano particle removal in brush scrubber cleaning. Applied Surface Science, 2011, 257, 3055-3062.	6.1	32
140	Enhancement of friction performance of fluorinated graphene and molybdenum disulfide coating by microdimple arrays. Carbon, 2020, 167, 122-131.	10.3	32
141	Radial-velocity profile along the surface of evaporating liquid droplets. Soft Matter, 2012, 8, 5797.	2.7	31
142	Exciton Radiative Recombination Dynamics and Nonradiative Energy Transfer in Two-Dimensional Transition-Metal Dichalcogenides. Journal of Physical Chemistry C, 2019, 123, 10087-10093.	3.1	31
143	A novel route to the synthesis of an Fe ₃ O ₄ /h-BN 2D nanocomposite as a lubricant additive. RSC Advances, 2019, 9, 6583-6588.	3.6	31
144	Ultrastable Lubricating Properties of Robust Self-Repairing Tribofilms Enabled by in Situ-Assembled Polydopamine Nanoparticles. Langmuir, 2020, 36, 852-861.	3.5	31

#	Article	IF	CITATIONS
145	Catalytically Active Oil-Based Lubricant Additives Enabled by Calcining Ni–Al Layered Double Hydroxides. Journal of Physical Chemistry Letters, 2020, 11, 113-120.	4.6	31
146	The Failure of Fluid Film at Nano-Scale. Tribology Transactions, 1999, 42, 912-916.	2.0	30
147	Extrusion formation mechanism on silicon surface under the silica cluster impact studied by molecular dynamics simulation. Journal of Applied Physics, 2008, 104, .	2.5	30
148	Analysis of Measurement Inaccuracy in Superlubricity Tests. Tribology Transactions, 2013, 56, 141-147.	2.0	30
149	Investigation of Protein Adsorption Mechanism and Biotribological Properties at Simulated Stem-Cement Interface. Journal of Tribology, 2013, 135, .	1.9	30
150	Molecular behaviors in thin film lubrication—Part two: Direct observation of the molecular orientation near the solid surface. Friction, 2019, 7, 479-488.	6.4	30
151	Macroscale superlubricity achieved between zwitterionic copolymer hydrogel and sapphire in water. Materials and Design, 2020, 188, 108441.	7.0	30
152	Superhigh-exfoliation graphene with a unique two-dimensional (2D) microstructure for lubrication application. Applied Surface Science, 2020, 513, 145608.	6.1	30
153	Preparation of α-alumina-g-polyacrylamide composite abrasive and chemical mechanical polishing behavior. Thin Solid Films, 2008, 516, 3005-3008.	1.8	29
154	Effects of Chemical Additives of CMP Slurry on Surface Mechanical Characteristics and Material Removal of Copper. Tribology Letters, 2012, 45, 309-317.	2.6	29
155	Material Removal Mechanism of Copper CMP from a Chemical–Mechanical Synergy Perspective. Tribology Letters, 2013, 49, 11-19.	2.6	29
156	Tribological properties of few-layer graphene oxide sheets as oil-based lubricant additives. Chinese Journal of Mechanical Engineering (English Edition), 2016, 29, 439-444.	3.7	29
157	Molecular behaviors in thin film lubrication—Part one: Film formation for different polarities of molecules. Friction, 2019, 7, 372-387.	6.4	29
158	Core–shell nanospheres to achieve ultralow friction polymer nanocomposites with superior mechanical properties. Nanoscale, 2019, 11, 8237-8246.	5.6	29
159	A molecular dynamics study of lubricating mechanism of graphene nanoflakes embedded in Cu-based nanocomposite. Applied Surface Science, 2020, 511, 145620.	6.1	29
160	Film forming characteristics of oil-in-water emulsion with super-low oil concentration. Colloids and Surfaces A: Physicochemical and Engineering Aspects, 2009, 340, 70-76.	4.7	28
161	Failure analysis of journal bearing used in turboset of a power plant. Materials & Design, 2013, 52, 923-931.	5.1	28
162	Experimental Investigation of Centrifugal Effects on Lubricant Replenishment in the Starved Regime at High Speeds. Tribology Letters, 2015, 59, 1.	2.6	28

#	Article	IF	CITATIONS
163	The film forming behavior at high speeds under oilâ^'air lubrication. Tribology International, 2015, 91, 6-13.	5.9	27
164	Superlubricity of 1,3-diketone based on autonomous viscosity control at various velocities. Tribology International, 2018, 126, 127-132.	5.9	27
165	Understanding Interlayer Contact Conductance in Twisted Bilayer Graphene. Small, 2020, 16, e1902844.	10.0	27
166	In situ synthesis of Mn3O4/graphene nanocomposite and its application as a lubrication additive at high temperatures. Applied Surface Science, 2021, 546, 149019.	6.1	27
167	Preparation and characterization of La2O3 doped diamond-like carbon nanofilms (I): Structure analysis. Diamond and Related Materials, 2007, 16, 1905-1911.	3.9	26
168	Combined effects of underlying substrate and evaporative cooling on the evaporation of sessile liquid droplets. Soft Matter, 2015, 11, 5632-5640.	2.7	26
169	Laser irradiation-induced laminated graphene/MoS ₂ composites with synergistically improved tribological properties. Nanotechnology, 2018, 29, 265704.	2.6	26
170	Influence of a carbon-based tribofilm induced by the friction temperature on the tribological properties of impregnated graphite sliding against a cemented carbide. Friction, 2021, 9, 686-696.	6.4	26
171	Micro-Bubble Phenomenon in Nanoscale Water-based Lubricating Film Induced by External Electric Field. Tribology Letters, 2008, 29, 169-176.	2.6	25
172	A highly tough and ultralow friction resin nanocomposite with crosslinkable polymer-encapsulated nanoparticles. Composites Part B: Engineering, 2020, 197, 108157.	12.0	25
173	Wear in-situ self-healing polymer composites incorporated with bifunctional microcapsules. Composites Part B: Engineering, 2022, 232, 109566.	12.0	25
174	Comparison of surface damage under the dry and wet impact: Molecular dynamics simulation. Applied Surface Science, 2011, 258, 1756-1761.	6.1	24
175	Experimental Investigation of Lubrication Film Starvation of Polyalphaolefin Oil at High Speeds. Tribology Letters, 2014, 56, 491-500.	2.6	24
176	Preparation of self-lubricating NiTi alloy and its self-adaptive behavior. Tribology International, 2019, 130, 43-51.	5.9	24
177	"Freezing―of Nanoconfined Fluids under an Electric Field. Langmuir, 2010, 26, 1445-1448.	3.5	23
178	Modification on the tribological properties of ceramics lubricated by water using fullerenol as a lubricating additive. Science China Technological Sciences, 2012, 55, 2656-2661.	4.0	23
179	Achievement of a near-perfect smooth silicon surface. Science China Technological Sciences, 2013, 56, 2847-2853.	4.0	23
180	Reduction of friction stress of ethylene glycol by attached hydrogen ions. Scientific Reports, 2014, 4, 7226.	3.3	23

#	Article	IF	CITATIONS
181	Graphene-induced reconstruction of the sliding interface assisting the improved lubricity of various tribo-couples. Materials and Design, 2020, 191, 108661.	7.0	23
182	Improvement of the lubrication properties of grease with Mn3O4/graphene (Mn3O4#G) nanocomposite additive. Friction, 2021, 9, 1361-1377.	6.4	23
183	Efficient one-pot synthesis of mussel-inspired Cu-doped polydopamine nanoparticles with enhanced lubrication under heavy loads. Chemical Engineering Journal, 2021, 426, 131287.	12.7	23
184	Fluctuation of Interfacial Electronic Properties Induces Friction Tuning under an Electric Field. Nano Letters, 2022, 22, 1889-1896.	9.1	23
185	Progress in material removal mechanisms of surface polishing with ultra precision. Science Bulletin, 2004, 49, 1687-1693.	1.7	22
186	Gas bubble phenomenon in nanoscale liquid film under external electric field. Applied Physics Letters, 2006, 89, 013104.	3.3	22
187	Mechanism of Superlubricity Conversion with Polyalkylene Glycol Aqueous Solutions. Langmuir, 2019, 35, 11784-11790.	3.5	22
188	Effect of surface charge on water film nanoconfined between hydrophilic solid surfaces. Journal of Applied Physics, 2009, 105, 124301.	2.5	21
189	Performance of Sodium Dodecyl Sulfate in Slurry with Glycine and Hydrogen Peroxide for Copper-Chemical Mechanical Polishing. Journal of the Electrochemical Society, 2010, 157, H1082.	2.9	21
190	Effect of liquid crystal molecular orientation controlled by an electric field on friction. Tribology International, 2017, 115, 477-482.	5.9	21
191	Layer-Number-Dependent Exciton Recombination Behaviors of MoS ₂ Determined by Fluorescence-Lifetime Imaging Microscopy. Journal of Physical Chemistry C, 2018, 122, 18651-18658.	3.1	21
192	Modeling Atomic-Scale Electrical Contact Quality Across Two-Dimensional Interfaces. Nano Letters, 2019, 19, 3654-3662.	9.1	21
193	XPS and ToF-SIMS analysis of the tribochemical absorbed films on steel surfaces lubricated with diketone. Tribology International, 2019, 130, 184-190.	5.9	21
194	Unraveling the Friction Evolution Mechanism of Diamondâ€Like Carbon Film during Nanoscale Runningâ€In Process toward Superlubricity. Small, 2021, 17, e2005607.	10.0	21
195	Influence of tribofilm on superlubricity of highly-hydrogenated amorphous carbon films in inert gaseous environments. Science China Technological Sciences, 2016, 59, 1795-1803.	4.0	20
196	Nanostructured tribolayer-dependent lubricity of graphene and modified graphene nanoflakes on sliding steel surfaces in humid air. Tribology International, 2020, 145, 106203.	5.9	20
197	Particles detection and analysis of hard disk substrate after cleaning of post chemical mechanical polishing. Applied Surface Science, 2009, 255, 9100-9104.	6.1	19
198	Modeling the Chemical-Mechanical Synergy during Copper CMP. Journal of the Electrochemical Society, 2011, 158, H197.	2.9	19

#	Article	lF	CITATIONS
199	Superlubricity of Si3N4 sliding against SiO2 under linear contact conditions in phosphoric acid solutions. Science China Technological Sciences, 2013, 56, 1678-1684.	4.0	19
200	Mechanical Properties and Interface Characteristics of Nanoporous Low- <i>k</i> Materials. ACS Applied Materials & Interfaces, 2014, 6, 13850-13858.	8.0	19
201	Chemical Mechanical Polishing of Stainless Steel as Solar Cell Substrate. ECS Journal of Solid State Science and Technology, 2015, 4, P162-P170.	1.8	19
202	Influence of annealing on the tribological properties of Zr-based bulk metallic glass. Journal of Non-Crystalline Solids, 2018, 481, 94-97.	3.1	19
203	Graphene Nanoflakes: Superlubricity of Graphite Induced by Multiple Transferred Graphene Nanoflakes (Adv. Sci. 3/2018). Advanced Science, 2018, 5, 1870018.	11.2	19
204	Inâ€Plane Potential Gradient Induces Low Frictional Energy Dissipation during the Stickâ€Slip Sliding on the Surfaces of 2D Materials. Small, 2019, 15, e1904613.	10.0	19
205	High-quality ultra-flat reduced graphene oxide nanosheets with super-robust lubrication performances. Chemical Engineering Journal, 2022, 438, 135620.	12.7	19
206	Mechanical properties of La2O3 doped diamond-like carbon films. Surface and Coatings Technology, 2008, 202, 1621-1627.	4.8	18
207	Modeling of particle removal processes in brush scrubber cleaning. Wear, 2011, 273, 105-110.	3.1	18
208	Reemulsification effect on the film formation of O/W emulsion. Journal of Colloid and Interface Science, 2014, 417, 238-243.	9.4	18
209	Investigation of film formation mechanism of oil-in-water (O/W) emulsions at high speeds. Tribology International, 2017, 109, 428-434.	5.9	18
210	Nonlinear Frictional Energy Dissipation between Silica-Adsorbed Surfactant Micelles. Journal of Physical Chemistry Letters, 2017, 8, 2258-2262.	4.6	18
211	Investigation of the lubrication properties and synergistic interaction of biocompatible liposome-polymer complexes applicable to artificial joints. Colloids and Surfaces B: Biointerfaces, 2019, 178, 469-478.	5.0	18
212	Modelling for water-based liquid lubrication with ultra-low friction coefficient in rough surface point contact. Tribology International, 2020, 141, 105901.	5.9	18
213	Dynamic wear sensor array based on single-electrode triboelectric nanogenerators. Nano Energy, 2020, 68, 104303.	16.0	18
214	Microscale superlubricity at multiple gold–graphite heterointerfaces under ambient conditions. Carbon, 2020, 161, 827-833.	10.3	18
215	Two-dimensional molybdenum carbide (MXene) as an efficient nanoadditive for achieving superlubricity under ultrahigh pressure. Friction, 2023, 11, 369-382.	6.4	18
216	Aminosilanization Nanoadhesive Layer for Nanoelectric Circuits with Porous Ultralow Dielectric Film. ACS Applied Materials & Interfaces, 2013, 5, 6097-6107.	8.0	17

#	Article	IF	CITATIONS
217	Passivation Kinetics of 1,2,4-Triazole in Copper Chemical Mechanical Polishing. ECS Journal of Solid State Science and Technology, 2016, 5, P272-P279.	1.8	17
218	Superlow Friction of Graphite Induced by the Self-Assembly of Sodium Dodecyl Sulfate Molecular Layers. Langmuir, 2017, 33, 12596-12601.	3.5	17
219	Film forming behavior in thin film lubrication at high speeds. Friction, 2018, 6, 156-163.	6.4	17
220	Fracture of the Intermolecular Hydrogen Bond Network Structure of Glycerol Modified by Carbon Nanotubes. Journal of Physical Chemistry C, 2018, 122, 19931-19936.	3.1	17
221	Controllable Interlayer Charge and Energy Transfer in Perovskite Quantum Dots/ Transition Metal Dichalcogenide Heterostructures. Advanced Materials Interfaces, 2019, 6, 1901263.	3.7	17
222	Water-based superlubricity in vacuum. Friction, 2019, 7, 192-198.	6.4	17
223	Fabrication of a graphene layer probe to measure force interactions in layered heterojunctions. Nanoscale, 2020, 12, 5435-5443.	5.6	17
224	Temporary or permanent liquid superlubricity failure depending on shear-induced evolution of surface topography. Tribology International, 2021, 161, 107076.	5.9	17
225	Effect of Nanoparticle Impact on Material Removal. Tribology Transactions, 2008, 51, 718-722.	2.0	16
226	Microstructure and mechanical properties of CeO2 doped diamond-like carbon films. Diamond and Related Materials, 2008, 17, 396-404.	3.9	16
227	Nanoparticle–wall collision in a laminar cylindrical liquid jet. Journal of Colloid and Interface Science, 2011, 359, 334-338.	9.4	16
228	Planarization process of single crystalline silicon asperity under abrasive rolling effect studied by molecular dynamics simulation. Applied Physics A: Materials Science and Processing, 2012, 109, 119-126.	2.3	16
229	<i>In situ</i> observation of the molecular ordering in the lubricating point contact area. Journal of Applied Physics, 2014, 116, .	2.5	16
230	Micro/atomic-scale vibration induced superlubricity. Friction, 2021, 9, 1163-1174.	6.4	16
231	Preparation and Tribological Properties of Self-Lubricating Epoxy Resins with Oil-Containing Nanocapsules. ACS Applied Materials & Interfaces, 2022, 14, 18954-18964.	8.0	16
232	Effect of microcontent of oil in water under confined condition. Applied Physics Letters, 2009, 95, 091908.	3.3	15
233	Energy transfer under impact load studied by molecular dynamics simulation. Journal of Nanoparticle Research, 2009, 11, 589-600.	1.9	15
234	A lubrication model between the soft porous brush and rigid flat substrate for post-CMP cleaning. Microelectronic Engineering, 2011, 88, 2862-2870.	2.4	15

#	Article	IF	CITATIONS
235	Measurement of the Friction between Single Polystyrene Nanospheres and Silicon Surface Using Atomic Force Microscopy. Langmuir, 2013, 29, 6920-6925.	3.5	15
236	Effects of interfacial alignments on the stability of graphene on Ru(0001) substrate. Applied Physics Letters, 2016, 108, .	3.3	15
237	An experimental investigation of double-side processing of cylindrical rollers using chemical mechanical polishing technique. International Journal of Advanced Manufacturing Technology, 2016, 82, 523-534.	3.0	15
238	Enhanced phase and amplitude image contrasts of polymers in bimodal atomic force microscopy. RSC Advances, 2017, 7, 11768-11776.	3.6	15
239	Interlayer interaction on twisted interface in incommensurate stacking MoS2: A Raman spectroscopy study. Journal of Colloid and Interface Science, 2019, 538, 159-164.	9.4	15
240	Progresses and problems in nano-tribology. Science Bulletin, 1998, 43, 369-378.	1.7	14
241	Film-forming Characteristics of Grease in Point Contact under Swaying Motions. Tribology Letters, 2009, 35, 57-65.	2.6	14
242	Bubble generation in a nanoconfined liquid film between dielectric-coated electrodes under alternating current electric fields. Applied Physics Letters, 2010, 96, .	3.3	14
243	Nanoconfined liquid aliphatic compounds under external electric fields: roles of headgroup and alkyl chain length. Soft Matter, 2011, 7, 4453.	2.7	14
244	Probing Particle Movement in CMP with Fluorescence Technique. Journal of the Electrochemical Society, 2011, 158, H681.	2.9	14
245	Influence of thermal effects on elastohydrodynamic (EHD) lubrication behavior at high speeds. Science China Technological Sciences, 2015, 58, 551-558.	4.0	14
246	Expressions for the evaporation of sessile liquid droplets incorporating the evaporative cooling effect. Journal of Colloid and Interface Science, 2016, 484, 291-297.	9.4	14
247	Preparation and tribological properties of PTFE/DE/ATF6 composites with self-contained solid-liquid synergetic lubricating performance. Composites Communications, 2020, 22, 100513.	6.3	14
248	Influence of elastic property on the friction between atomic force microscope tips and 2D materials. Nanotechnology, 2020, 31, 285710.	2.6	14
249	Influence of structural evolution on sliding interface for enhancing tribological performance of onion-like carbon films via thermal annealing. Applied Surface Science, 2021, 541, 148441.	6.1	14
250	Insight into the formation mechanism of durable hexadecylphosphonic acid bilayers on titanium alloy through interfacial analysis. Colloids and Surfaces A: Physicochemical and Engineering Aspects, 2014, 447, 51-58.	4.7	13
251	Speed dependence of liquid superlubricity stability with H ₃ PO ₄ solution. RSC Advances, 2017, 7, 49337-49343.	3.6	13
252	Controllable Superlubricity System of Polyalkylene Glycol Aqueous Solutions under Various Applied Conditions. Macromolecular Materials and Engineering, 2020, 305, 2000141.	3.6	13

#	Article	IF	CITATIONS
253	A smart healable anticorrosion coating with enhanced loading of benzotriazole enabled by ultra-highly exfoliated graphene and mussel-inspired chemistry. Carbon, 2022, 187, 439-450.	10.3	13
254	Electrospreading of dielectric liquid menisci on the small scale. Soft Matter, 2011, 7, 6076.	2.7	12
255	Preparation of poly (N-isopropylacrylamide) brush bonded on silicon substrate and its water-based lubricating property. Science China Technological Sciences, 2012, 55, 3352-3358.	4.0	12
256	Optimization of design of experiment for chemical mechanical polishing of a 12-inch wafer. Microelectronic Engineering, 2013, 112, 5-9.	2.4	12
257	Linear growth of colloidal rings at the edge of drying droplets. Colloids and Surfaces A: Physicochemical and Engineering Aspects, 2014, 447, 28-31.	4.7	12
258	Investigation of ultra-low friction on steel surfaces with diketone lubricants. RSC Advances, 2018, 8, 9402-9408.	3.6	12
259	Magnetic field effect on apparent viscosity reducing of different crude oils at low temperature. Colloids and Surfaces A: Physicochemical and Engineering Aspects, 2021, 629, 127372.	4.7	12
260	Synergistic Effect of Ethylene Thiourea and Bis-(3-sulfopropyl)-disulfide on Acid Cu Electrodeposition. Journal of the Electrochemical Society, 2007, 154, D526.	2.9	11
261	The Film Behaviors of Grease in Point Contact During Microoscillation. Tribology Letters, 2010, 38, 259-266.	2.6	11
262	Experimental Investigation of Lubrication Properties at High Contact Pressure. Tribology Letters, 2010, 40, 85-97.	2.6	11
263	Thin liquid film lubrication under external electrical fields: Roles of liquid intermolecular interactions. Journal of Applied Physics, 2011, 109, .	2.5	11
264	The Role of Hydroxyethyl Cellulose (HEC) in the Chemical Mechanical Planarization of Copper. Journal of the Electrochemical Society, 2012, 159, H329-H334.	2.9	11
265	Damages on the lubricated surfaces in bearings under the influence of weak electrical currents. Science China Technological Sciences, 2013, 56, 2979-2987.	4.0	11
266	Effect of Alkyl Chain Length on the Orientational Behavior of Liquid Crystals Nano-Film. Tribology Letters, 2016, 62, 1.	2.6	11
267	Triboluminescence modulated by humidity. Journal of Luminescence, 2017, 182, 22-28.	3.1	11
268	Gradual degeneration of liquid superlubricity: Transition from superlubricity to ordinary lubrication, and lubrication failure. Tribology International, 2019, 130, 352-358.	5.9	11
269	Potential-Dependent Friction on a Graphitic Surface in Ionic Solution. Journal of Physical Chemistry C, 2020, 124, 23745-23751.	3.1	11
270	Achieving a superlubricating ohmic sliding electrical contact <i>via</i> a 2D heterointerface: a computational investigation. Nanoscale, 2020, 12, 7857-7863.	5.6	11

#	Article	IF	CITATIONS
271	Effect of deformation modes and heat treatment on microstructure and impact property restoration of internal crack healing in SA 508 steel. Materials Science & Engineering A: Structural Materials: Properties, Microstructure and Processing, 2020, 778, 139073.	5.6	11
272	THIN FILM LUBRICATION AND LUBRICATION MAP. Jixie Gongcheng Xuebao/Chinese Journal of Mechanical Engineering, 2000, 36, 5.	0.5	11
273	Tribological properties of La2O3 and CeO2 doped CoCrW coatings deposited by supersonic plasma spraying. Science Bulletin, 2007, 52, 3292-3298.	1.7	10
274	Phase transformation during silica cluster impact on crystal silicon substrate studied by molecular dynamics simulation. Nuclear Instruments & Methods in Physics Research B, 2008, 266, 3231-3240.	1.4	10
275	Dynamic phase transformation of crystalline silicon under the dry and wet impact studied by molecular dynamics simulation. Journal of Applied Physics, 2010, 108, .	2.5	10
276	Direct observation on the behaviour of emulsion droplets and formation of oil pool under point contact. Applied Physics Letters, 2012, 101, .	3.3	10
277	Effect of pH on the liquid superlubricity between Si ₃ N ₄ and glass achieved with phosphoric acid. RSC Advances, 2014, 4, 45735-45741.	3.6	10
278	Ultra-low friction achieved by diluted lactic acid solutions. RSC Advances, 2014, 4, 28860.	3.6	10
279	Friction Anisotropy Induced by Oriented Liquid Crystal Molecules. Tribology Letters, 2016, 61, 1.	2.6	10
280	Studies on triboluminescence emission characteristics of various kinds of bulk ZnS crystals. Journal of Luminescence, 2017, 186, 307-311.	3.1	10
281	Influence of interface interaction on the moiré superstructures of graphene on transition-metal substrates. RSC Advances, 2017, 7, 12179-12184.	3.6	10
282	Effect of Parameters on Internal Crack Healing in 30Cr2Ni4MoV Steel for 600-Ton Ultra-Super Ingots. Metals, 2017, 7, 149.	2.3	10
283	Water molecules on the liquid superlubricity interfaces achieved by phosphoric acid solution. Biosurface and Biotribology, 2018, 4, 94-98.	1.5	10
284	Investigation on inner flow field characteristics of groove textures in fully lubricated thrust bearings. Industrial Lubrication and Tribology, 2018, 70, 754-763.	1.3	10
285	Cationic Surfactant Micelles Lubricate Graphitic Surface in Water. Langmuir, 2019, 35, 11108-11113.	3.5	10
286	Macroscale Light-Controlled Lubrication Enabled by Introducing Diarylethene Molecules in a Nanoconfinement. Langmuir, 2020, 36, 5820-5828.	3.5	10
287	Effects of surface physicochemical properties on the tribological properties of liquid paraffin film in the nanoscale. Surface and Interface Analysis, 2001, 32, 286-288.	1.8	9
288	Analysis on contact and flow features in CMP process. Science Bulletin, 2006, 51, 2281-2286.	1.7	9

#	Article	IF	CITATIONS
289	Luminescence of carbon nanotube bulbs. Science Bulletin, 2007, 52, 113-117.	1.7	9
290	Effects of the Polishing Variables on the Wafer-Pad Interfacial Fluid Pressure in Chemical Mechanical Polishing of 12-Inch Wafer. Journal of the Electrochemical Society, 2012, 159, H342-H348.	2.9	9
291	Water droplets on a hydrophobic insulator surface under high voltages: A thermal perspective. Applied Physics Letters, 2012, 101, 131602.	3.3	9
292	Effects of pH and Oxidizer on Chemical Mechanical Polishing of AISI 1045 Steel. Tribology Letters, 2014, 56, 327-335.	2.6	9
293	Pitted Surfaces Produced by Lactic Acid Lubrication and Their Effect on Ultra-Low Friction. Tribology Letters, 2015, 57, 1.	2.6	9
294	Band Structure, Band Offsets, and Intrinsic Defect Properties of Few-Layer Arsenic and Antimony. Journal of Physical Chemistry C, 2020, 124, 7441-7448.	3.1	9
295	Macroscale superlubricity under ultrahigh contact pressure in the presence of layered double hydroxide nanosheets. Nano Research, 2022, 15, 4700-4709.	10.4	9
296	Tribological properties of OTS self-assembled monolayers. Science Bulletin, 2001, 46, 698-701.	1.7	8
297	Effect of solid surface on the formation of thin confined lubricating film of water with micro-content of oil. Applied Surface Science, 2010, 256, 6574-6579.	6.1	8
298	"Boiling―in the water evaporating meniscus induced by Marangoni flow. Applied Physics Letters, 2012, 101, .	3.3	8
299	Advances in thin film lubrication (TFL): From discovery to the aroused further researches. Science China Technological Sciences, 2015, 58, 1609-1616.	4.0	8
300	Effect of Potassium Ions on Tantalum Chemical Mechanical Polishing in H ₂ O ₂ -Based Alkaline Slurries. ECS Journal of Solid State Science and Technology, 2016, 5, P100-P111.	1.8	8
301	Tunable lubricity of aliphatic ammonium graphite intercalation compounds at the micro/nanoscale. Carbon, 2017, 115, 574-583.	10.3	8
302	Nano-Ag-forest based surface enhanced Raman spectroscopy (SERS) of confined acetic acid. Colloids and Surfaces A: Physicochemical and Engineering Aspects, 2018, 547, 126-133.	4.7	8
303	Improvement of Load Bearing Capacity of Nanoscale Superlow Friction by Synthesized Fluorinated Surfactant Micelles. ACS Applied Nano Materials, 2018, 1, 953-959.	5.0	8
304	Atomic Scale Simulation on the Anti-Pressure and Friction Reduction Mechanisms of MoS2 Monolayer. Materials, 2018, 11, 683.	2.9	8
305	Exploring interlayer interaction of SnSe2 by low-frequency Raman spectroscopy. Physica E: Low-Dimensional Systems and Nanostructures, 2019, 105, 7-12.	2.7	8
306	Achieving controllable friction of ultrafine-grained graphite HPG510 by tailoring the interfacial nanostructures. Applied Surface Science, 2020, 512, 145731.	6.1	8

#	Article	IF	CITATIONS
307	Dynamic friction energy dissipation and enhanced contrast in high frequency bimodal atomic force microscopy. Friction, 2022, 10, 748-761.	6.4	8
308	Coupled Optimization of Groove Texture for Parallel Ring–Ring Friction Pairs: Theory and Experiments. Tribology Letters, 2022, 70, 1.	2.6	8
309	The experimental rules of mica as a reference sample of AFM/FFM measurement. Science Bulletin, 2001, 46, 349-352.	1.7	7
310	A PIV system for two-phase flow with nanoparticles. International Journal of Surface Science and Engineering, 2008, 2, 168.	0.4	7
311	Electric-fields-enhanced destabilization of oil-in-water emulsions flowing through a confined wedgelike gap. Journal of Applied Physics, 2010, 108, 064314.	2.5	7
312	Motor Power Signal Analysis for End-Point Detection of Chemical Mechanical Planarization. Micromachines, 2017, 8, 177.	2.9	7
313	Hot Deformation Behavior of As-Cast 30Cr2Ni4MoV Steel Using Processing Maps. Metals, 2017, 7, 50.	2.3	7
314	Normal and Frictional Force Hysteresis between Selfâ€Assembled Fluorosurfactant Micelle Arrays at the Nanoscale. Advanced Materials Interfaces, 2018, 5, 1700802.	3.7	7
315	The effect of magnetic field on the hydration of cation in solution revealed by THz spectroscopy and MDs. Colloids and Surfaces A: Physicochemical and Engineering Aspects, 2019, 582, 123822.	4.7	7
316	Lubricity and Adsorption of Castor Oil Sulfated Sodium Salt Emulsion Solution on Titanium Alloy. Tribology Letters, 2019, 67, 1.	2.6	7
317	Study on microstructural and tribological properties of sulphonitrocarburized layers diffused by hollow cathode discharging. Vacuum, 2020, 174, 109188.	3.5	7
318	Thermal-mechanical fully coupled analysis of high-speed angular contact ball bearings. Journal of Mechanical Science and Technology, 2021, 35, 669-678.	1,5	7
319	The relationship between surface structure and super-lubrication performance based on 2D MOFs. Applied Materials Today, 2022, 26, 101382.	4.3	7
320	Stress analysis of Cu/low-k interconnect structure during whole Cu-CMP process using finite element method. Microelectronics Reliability, 2013, 53, 767-773.	1.7	6
321	AC Pulse Dielectric Barrier Corona Discharge Over Oil Surfaces: Effect of Oil Temperature. IEEE Transactions on Plasma Science, 2013, 41, 481-484.	1.3	6
322	Investigation on the galvanic corrosion of copper during chemical mechanical polishing of ruthenium barrier layer. , 2014, , .		6
323	Dynamical characterization of micro cantilevers by different excitation methods in dynamic atomic force microscopy. Review of Scientific Instruments, 2018, 89, 115109.	1.3	6
324	Crack Healing and Mechanical Properties Recovery in SA 508–3 Steel. Materials, 2019, 12, 890.	2.9	6

#	Article	IF	CITATIONS
325	Coupling effect of boundary tribofilm and hydrodynamic film. Cell Reports Physical Science, 2022, 3, 100778.	5.6	6
326	Tribological and compressive creep properties of polytetrafluoroethylene/nickelâ€ŧitanium shape memory alloy composites. Polymer Composites, 0, , .	4.6	6
327	Spread of double-walled carbon nanotube membrane. Science Bulletin, 2007, 52, 997-1000.	1.7	5
328	Investigation on growth process and tribological behavior of mixed alkylsilane self-assembled molecular films in aqueous solution. Applied Surface Science, 2012, 258, 8533-8537.	6.1	5
329	Wafer bending/orientation characterization and their effects on fluid lubrication during chemical mechanical polishing. Tribology International, 2013, 66, 330-336.	5.9	5
330	Direct observation of the formation and destruction of the inverted continuous oil phase in the micro-outlet region achieved by the confined diluted O/W emulsion stream. Soft Matter, 2014, 10, 7946-7951.	2.7	5
331	Interfacial Dynamics and Adhesion Behaviors of Water and Oil Droplets in Confined Geometry. Langmuir, 2014, 30, 7695-7702.	3.5	5
332	Interfacial interaction and enhanced image contrasts in higher mode and bimodal mode atomicÂforce microscopy. RSC Advances, 2017, 7, 55121-55130.	3.6	5
333	Signal processing and analysis for copper layer thickness measurement within a large variation range in the CMP process. Review of Scientific Instruments, 2017, 88, 115103.	1.3	5
334	Different directional energy dissipation of heterogeneous polymers in bimodal atomic force microscopy. RSC Advances, 2019, 9, 27464-27474.	3.6	5
335	Analysis on mechanism of thin film lubrication. Science Bulletin, 2005, 50, 2645-2649.	1.7	4
336	Effect of crystallographic orientation on the extrusion of silicon surface during an impact: Molecular dynamics simulation. Nuclear Instruments & Methods in Physics Research B, 2012, 270, 133-139.	1.4	4
337	The Assessment of Interface Adhesion of Cu/Ta/Black Diamondâ,,¢/Si Films Stack Structure by Nanoindentation and Nanoscratch Tests. Tribology Letters, 2014, 53, 401-410.	2.6	4
338	Guest editorial: Special issue on superlubricity. Friction, 2014, 2, 93-94.	6.4	4
339	Size and shape controllable preparation of graphene sponge by freezing, lyophilizing and reducing in container. Science China Technological Sciences, 2016, 59, 709-713.	4.0	4
340	Imaging contrast and tip-sample interaction of non-contact amplitude modulation atomic force microscopy withQ-control. Journal Physics D: Applied Physics, 2017, 50, 415307.	2.8	4
341	The Effects of Homogenizing and Quenching and Tempering Treatments on Crack Healing. Metals, 2020, 10, 427.	2.3	4
342	Light-Controlled Friction by Carboxylic Azobenzene Molecular Self-Assembly Layers. Frontiers in Chemistry, 2021, 9, 707232.	3.6	4

#	Article	IF	CITATIONS
343	Preparation of Triple-Functionalized Montmorillonite Layers Promoting Thermal Stability of Polystyrene. Nanomaterials, 2021, 11, 2170.	4.1	4
344	Characteristics of thin liquid film under an external electric field. Tribology International, 2007, 40, 1718-1723.	5.9	3
345	Study of lubrication behavior of pure water for hydrophobic friction pair. Science in China Series D: Earth Sciences, 2009, 52, 3128-3134.	0.9	3
346	A comparative study of tribological properties between perfluoro and non-perfluoro alkylsilane self-assembled monolayers(SAMs). Journal Wuhan University of Technology, Materials Science Edition, 2009, 24, 588-593.	1.0	3
347	Preparation, Characterization and Formation Mechanism of Thermoplastic Polyurethane Nanostructures Using Solution Wetting Template. Journal of Nanoscience and Nanotechnology, 2011, 11, 10240-10246.	0.9	3
348	Direct observation of oil displacement by water flowing toward an oil nanogap. Journal of Applied Physics, 2011, 110, 044906.	2.5	3
349	Atomic Scale Simulation on the Fracture Mechanism of Black Phosphorus Monolayer under Indentation. Nanomaterials, 2018, 8, 682.	4.1	3
350	Superlubricity with nonaqueous liquid. , 2021, , 379-403.		3
351	Extremely low friction on gold surface with surfactant molecules induced by surface potential. Friction, 2023, 11, 513-523.	6.4	3
352	Controllable group tailoring enables enhanced pH-responsive behaviors of polydopamine delivery system in smart self-healing anticorrosion coatings. Progress in Organic Coatings, 2022, 170, 106989.	3.9	3
353	Tribology in Nanomanufacturing—Interaction between Nanoparticles and a Solid Surface. , 2009, , 5-10.		2
354	Influence of pH, immersion time, and benzotriazole concentration on copper corrosion in citric acid based slurries. Science Bulletin, 2011, 56, 1158-1164.	1.7	2
355	Electrical potential modulation of dynamic film properties of aqueous surfactant solutions through a nanogap. Journal of Applied Physics, 2011, 109, 024309.	2.5	2
356	A flexible nanobrush pad for the chemical mechanical planarization of Cu/ultra-low-к materials. Nanoscale Research Letters, 2012, 7, 603.	5.7	2
357	Interface characteristics of thin liquid films in a charged lubricated contact. Surface and Interface Analysis, 2015, 47, 315-324.	1.8	2
358	Triboluminescence dominated by crystallographic orientation. Scientific Reports, 2016, 6, 26324.	3.3	2
359	Self-Retraction of Surfactant Droplets on a Superhydrophilic Surface. Langmuir, 2018, 34, 15388-15395.	3.5	2
360	Thinning of glycerol in the presence of multi-walled carbon nanotubes. Journal of Chemical Physics, 2019, 151, 054302.	3.0	2

#	Article	IF	CITATIONS
361	Temperature measurement during the sliding between Al2O3 and SiO2 crystals by double line of Atomic Emission Spectroscopy. Journal of Luminescence, 2019, 215, 116615.	3.1	2
362	A simple method to understand molecular conformation on surface-enhanced Raman scattering substrate. Journal of Molecular Structure, 2021, 1223, 128908.	3.6	2
363	The transients in the evaporation of sessile liquid droplets and the applicability of the steady-state approximation. International Journal of Heat and Mass Transfer, 2021, 169, 120946.	4.8	2
364	Influence of "Seebeck effect" on charge transfer between two friction surfaces. Tribology International, 2021, 161, 107060.	5.9	2
365	Friction Process of Superlubricity. , 2012, , .		1
366	Film formation of yogurt under confined condition. Surface and Interface Analysis, 2012, 44, 258-262.	1.8	1
367	Guest editorial: Special issue on thin film lubrication. Friction, 2016, 4, 277-279.	6.4	1
368	Increased Film Thickness of Oil-in-Water (O/W) Emulsions at High Speed. Tribology Letters, 2017, 65, 1.	2.6	1
369	Dramatically Enhanced Film-Formation Performance Using O/W Emulsion Under Starving Feeding Mode. Tribology Letters, 2017, 65, 1.	2.6	1
370	Revealing the essence of luminescence energy transformation from silica surfaces. Journal of Luminescence, 2018, 197, 389-395.	3.1	1
371	Tangential motion mechanism and reverse hydrodynamic effects of acoustic platform with nonparallel squeeze film. Proceedings of the Institution of Mechanical Engineers, Part J: Journal of Engineering Tribology, 2019, 233, 194-204.	1.8	1
372	Tribo-Induced Near-Infrared Light Emission between Metal and Quartz. Langmuir, 2020, 36, 1165-1173.	3.5	1
373	Toward micro- and nanoscale robust superlubricity by 2D materials. , 2021, , 131-144.		1
374	Liquid superlubricity with 2D material additives. , 2021, , 167-187.		1
375	Superlubricity of water-based lubricants. , 2021, , 333-357.		1
376	Visualizing ultrafast defectâ€controlled interlayer electronâ€phonon coupling in van der Waals heterostructures. Advanced Materials, 2022, , 2106955.	21.0	1
377	Light-induced Current in Long Carbon Nanotubes. ECS Transactions, 2006, 2, 85-92.	0.5	0

The Film Formation Mechanism of High Water-Based Emulsions. , 2010, , .

0

#	Article	IF	CITATIONS
379	Superlubricity Mechanism of Brasenia Schreberi Mucilage. , 2012, , .		0
380	Behavior of O/W Emulsion Under Point Contact. , 2012, , .		0
381	Tip-induced nanoreactor for silicate. Scientific Reports, 2015, 5, 14039.	3.3	0
382	Guest editorial: Special issue on 6th World Tribology Congress. Friction, 2017, 5, 231-232.	6.4	0
383	Vibration-induced superlubricity. , 2021, , 53-70.		0
384	Energy dissipation through phonon and electron behaviors of superlubricity in 2D materials. , 2021, , 145-166.		0
385	Tribo-induced interfacial nanostructures stimulating superlubricity in amorphous carbon films. , 2021, , 289-307.		0
386	Exploration of molecular behaviors in liquid superlubricity. , 2021, , 475-498.		0
387	Superlubricity of black phosphorus as lubricant additive. , 2021, , 439-460.		0
388	Temperature-controlled Friction Coefficient Lubricated by Liquid Crystal. Liquid Crystals, 2022, 49, 66-71.	2.2	0
389	Fast Opticalâ€Thermal Responsive Intelligent Glass Realized by Hydrated Poly(N â€Isopropylacrylamide) Film. Macromolecular Materials and Engineering, 2021, 306, 2100272.	3.6	0
390	Advancements and Future of Tribology from IFToMM. Mechanisms and Machine Science, 2011, , 203-219.	0.5	0